

NIMS (Negative Index Möbius Strips): Resonator for Next Generation Electronic Signal Sources

Ajay K. Poddar

Synergy Microwave, NJ, USA

Ulrich L. Rohde

BTU Cottbus, Munich, Germany

Ignaz Eisele

EMFT, Munich, Germany

Enrico Rubiola

FEMTO-ST Institute, France

Abstract—A novel NIMO (Negative Index Möbius Oscillator) circuit is reported for application in current and later generation communication systems. The NIMO circuit uses NIMS (negative index möbius strips) resonator for improving PN (phase noise) and FOM (figure of merit). The measured PN @ 10 kHz offset from the carrier frequency 28.5 GHz is -122 dBc/Hz with typical 10.56 dBm O/P power and 680 mW DC power consumption. The measured FOM for a 28.5 GHz signal source at 1 MHz offset is -226 dBc/Hz. The reported NIMO topology enables next generation energy-efficient signal source solutions in monolithic integrated circuit and surface mounted planar technology.

Keywords— Möbius-Strips Metamaterial, NIMS, NIMO, PN

I. INTRODUCTION

Negative Index Möbius-Strips (NIMS) has captured the interest of research scientists because of distinctive properties, such as topological symmetry (property, conserved when the system undergoes an alteration (deformation, twisting and stretching of objects) and negative index ($n = -\sqrt{\epsilon\mu}$; $\epsilon < 0$, $\mu < 0$) characteristics. Figure (1) shows the typical negative index ($\epsilon < 0$, $\mu < 0$) Möbius-Strips formed Grapheme nanoribbons, which possess topology-induced desirable high Q-factor components and desirable electromagnetic properties. Unlike conventional materials, which interact with EM (electromagnetic) wave based on their chemical composition, the properties of NIM (negative index material), known as Metamaterial come from their geometric topology structure.

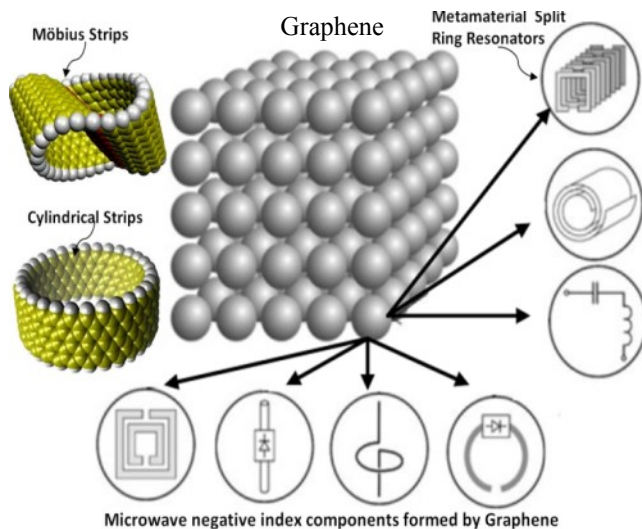


Fig.1: Möbius-Strips structure formed by Grapheme nanoribbons exhibits negative index properties ($\epsilon < 0$, $\mu < 0$), well suited suitable for high quality factor microwave frequency components

NIMs (Negative Index Materials) are artificial engineered topological structures illustrated in Figure (1), intended to modify the bulk permeability and permittivity of the medium, which can be realized by placing periodically unit cell NIM's structures under the constraints of their size (typically much less than the wavelength of incident EM wave). It is interesting to note that by changing the position, orientation, excitation of NIM's structure, important parameters (permittivity, permeability, refractive index, transmission, reflection, impedance, and coupling) can be tuned and optimized for desired applications. There are many ways to vary the properties of NIM, such as by using ferrites, liquid crystals, frequency-selective surfaces, and manipulating the lattice structure; but these methods are band limited [1]-[20].

Figure (2) shows the typical characteristics of the medium that explains the properties of natural and artificial engineered composite material [1]. As shown in Figure (2), the third quadrant describes the properties of left-handed medium that posses NIM (negative index material: $n = -\sqrt{\epsilon\mu}$; $\epsilon < 0$, $\mu < 0$) characteristics. The evanescent-mode energy storing and resonant characteristics of the third-quadrant material enables potential applications in electronics, medical, space, and optics. Hence, it is important to understand the fundamental EM dynamics of the third-quadrant material ($\epsilon < 0$, $\mu < 0$) for designing NIMS resonator based electronic signal sources. It is important to note that exact characterization of ϵ and μ of NIM structure is challenging task for wideband frequency operation.

While it is possible to characterize the NIM's in terms of refractive index (n) and normalized impedance (z) but these do not provide meaningful information. The ongoing effort by research scientists is to categorize NIM-structure by effective constitutive parameters: $\epsilon_r = n/z$, $\mu_r = n \times z$, which gives a direct and an understandable interpretation of medium such as NIMs.

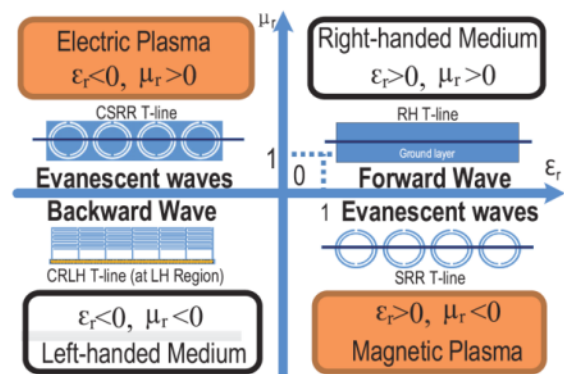


Fig. 2: A typical representation of the medium: 3rd quadrant explains left-handed medium, NIM (negative index) material properties [1]

In addition to this, the justification of using effective constitutive parameters ($\epsilon < 0$, $\mu < 0$) provide a convenient means to understand the behavior of the artificial engineered NIMs structures without considering in details about the local EM-field distribution. To establish the faithful values of these effective constitutive parameters, numerous methods reported, but none of them provides exact solutions due to hypothesis of NIM's tiny size and neglecting the couplings [1]-[27]. The general isotropic medium model assumes that the induced electric and magnetic dipoles are mutually independent, but in reality this is not always the case. NIMs are intrinsically anisotropic and sometime bianisotropic because of geometry and orientations of their structure. For example, SRs as shown in Figure (3), typically used in NIMs, exhibit simultaneous electric and magnetic response, i.e., corresponding dipoles are coupled [5]. This leads to cross-coupling between electric and magnetic field in SR inspired NIM structures. Therefore, it is not recommended to discount the magneto-electric coupling that depends on shape of inclusions, wave- polarizations, excitation, and orientation of NIM's structures. To account for both asymmetric reflection and magneto-electrical coupling, bianisotropic medium model can be used.

Figure (3) shows the typical circular and square split ring structures for the realization of NIM (negative index material), the size of SRs (split rings) and the distances between them are kept smaller than the wavelength (λ). Under this assumption, SR-NIM structure may present bulk properties and can be characterized by a macroscopic model, with effective index parameter (ϵ and μ). The expression for index (n) is given by

$$n = \pm\sqrt{(\pm\epsilon)(\pm\mu)} = \pm\sqrt{\mu\epsilon} \quad (1)$$

From (1), the positive sign is used for n when $\epsilon, \mu > 0$, whereas the negative sign is used when $\epsilon, \mu < 0$. The assumption of positive index ($n > 0$) implies that the index n is a scalar, and does not depend on frequency. But in reality, this is not always true. The energy of the field (W) would be negative ($W = \epsilon E^2 + \mu H^2$) value when ϵ and μ are negative, and this is not possible, hence ϵ and μ bound to depend on frequency and fall into complex domain [2]. The unified expression of energy W can be described by

$$W = \frac{\partial(\omega\epsilon)}{\partial\omega} E^2 + \frac{\partial(\omega\mu)}{\partial\omega} H^2 \quad (2)$$

where $\epsilon(\omega) = \epsilon'(\omega) + j\epsilon''(\omega)$ and $\mu(\omega) = \mu'(\omega) + j\mu''(\omega)$. From (2), the electrodynamics of negative index materials ($n < 0$; $\epsilon < 0$ and $\mu < 0$) would give positive value of W for a very broad class of dispersive material characterized by $\epsilon(\omega)$ and $\mu(\omega)$, exhibit dependency on frequency.

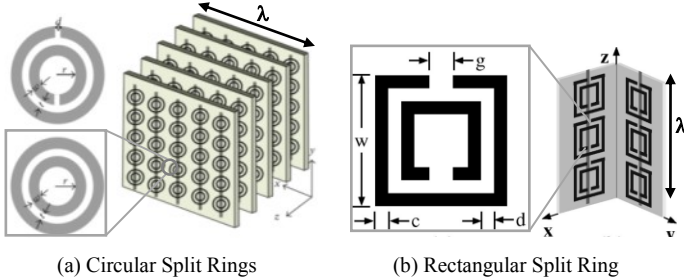


Fig. 3: Shows the typical SRRs and the construction of NIM with closed SRR wire structure: (a) Circular Split Ring, and (b) Rectangular Split Ring

Any material supporting single propagating mode at a known frequency, usually exhibits well-defined index (n), despite the material is homogeneous/continuous or not. But it is not easy to assign normalized impedance (z) to a non-homogeneous material, because z strongly depends on surface termination and overall size of the material [1]. The classical homogenization theories are typically valid when the unit-cell size is insignificant with respect to the wavelength (the zero frequency limits) and thus might be expected to result in a poor description of negative index materials. The key supposition is, if the wavelength of the incident wave is much larger than the size and spacing between the NIM's unit cell element then it is possible to perform homogenization, and to obtain a approved value of z within an acceptable limit of errors [2]-[3].

Assuming the size of NIM's structure is much smaller than $\lambda/10$, homogenization theory can be applied to topology inspired Möbius Strips structure, averaging of Maxwell's equations over small volumes (with respect to wavelength) can be performed to get analogous uniform continuous harmonized medium, described by effective constitutive parameters (ϵ and μ). It is possible to retrieve values for the complex refractive index (n) and wave impedance (z) of inhomogeneous periodic NIMS structure, by prior information about termination of the NIMS-unit cell structure, phases and amplitudes of the waves transmitted/reflected from the NIMS sample. But the challenge is if the NIMS structures are not symmetric along the wave propagation direction, 2-different values of impedance (z) are retrieved corresponding to 2-incident directions of propagation. This ambiguity in the computation of impedance (z) leads to a fundamental ambiguity in the definitions of ϵ and μ for MIMS, which increases as the ratio of NIMS unit cell dimension to wavelength increases.

The simplest approach of theoretical formulation of SR inspired NIM (negative index material) can be deduced from equivalent circuit model that gives insight into the relationship between the physical properties and geometrical parameters of SRRs as shown in Figures (3) and (4). The analytical values of constitutive parameters (ϵ_{zz} , μ_{yy} , ξ_0) is given by [5, 13, 17]

$$\epsilon_z = 1 + \frac{1}{\epsilon_0 a^3} \left\{ \epsilon_0 \frac{16}{3} r_{ext}^3 + 4 d_{eff}^2 r_0^2 C_{pull}^2 L \left(\frac{\omega^2}{\omega_0^2 - \omega^2 - i\omega\gamma} \right) \right\} \quad (3)$$

$$\mu_y = 1 + \frac{\mu_0}{a^3} \left\{ \frac{\pi^2 r_0}{L} \left(\frac{\omega^2}{\omega_0^2 - \omega^2 - i\omega\gamma} \right) \right\} \quad (4)$$

$$\xi_0 = -i \sqrt{\frac{\mu_0}{\epsilon_0 a^3}} \left\{ -2 i r_0^3 d_{eff} C_{pull} \frac{\omega_0^2}{\omega} \left(\frac{\omega^2}{\omega_0^2 - \omega^2 - i\omega\gamma} \right) \right\} \quad (5)$$

where $d_{eff} = c + s$, $\gamma = \frac{R}{L}$, $r_0 = r + c + s/2$ and $r_{ext} = r + 2c + s$; L and C_{pull} are the total inductance of the SRR and the capacitance between the rings respectively. From the equivalent circuit model, RR behaves as a resonant LC circuit, and that the frequency of the resonance is given by

$$\omega_0^2 = \frac{1}{\left(\frac{1}{2} \pi r_0 C_{pull} + C_{gap} \right) L} \quad (6)$$

L and C_{pull} can be calculated from the analytical equations reported in [17]. C_{gap} is the capacitance of the gap, if the gap is narrow, its capacitance can be analytically written as [18]

$$C_{gap} = \frac{\epsilon_0 c h}{g} + C_0 \text{ with } C_0 = \epsilon_0 (h + c + g) \quad (7)$$

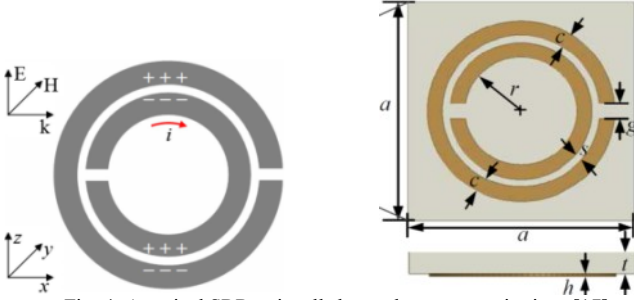


Fig. 4: A typical SRR unit cell shows the asymmetric rings [17]

As shown in Figure (4), for example, the dimension of SRR is given as $a = 3$ mm, $r = 0.74$ mm, $c = 0.2$ mm, $s = 0.1$ mm, $g = 0.2$ mm, $t = 0.3$ mm, $h = 35$ μ m and permittivity of the substrate is $\epsilon_0 \cdot 8.8541 \times 10^{-12}$ F/m. From (3)-(7), $L = 3.9287 \times 10^{-9}$ H, $C_{\text{pul}} = 1.6806 \times 10^{-11}$ F, $C_{\text{gap}} = 4.155 \times 10^{-15}$ F and $R = 0.4901$ Ω at the frequency of resonance. The numerical values obtained using (3)-(7) are approximate. Therefore, poor accuracy of analytical method and the deficiency of complex models for thicker structures limit its substantiation. The alternative approach is retrieval technique based on extraction of S-parameters. The advantages of retrieval method are it can be used for simulated and measured S-parameter data; thin samples (in the propagation direction) are preferred to minimize the errors.

There are three imperative methods generally used for the determination of effective constitutive parameters based on applications and acceptable limit of errors [3]. The first method is to numerically calculate the ratios of the EM (electromagnetic) field inside NIM's structure but this approach is good for numerical simulations, and not appropriate for experimental measurement [4]. The second method calculates the effective constitutive parameters by using analytical models of NIM's structures including numerical averaging of fields. But this technique is not suitable for complex NIM's structures such as NIMS [5]. The third method is a retrieval technique based on the inversion of scattering data (S-parameters) of a finite slab, called the NRW (Nicolson–Ross–Weir) procedure [6]-[7]. NRW method was developed for the measurements of complex permittivity and permeability of natural materials, recently applied to NIMS (negative index materials).

The problem with NRW method arises in case when topology driven NIM's structure undergo asymmetric reflections. Smith *et al.* [2] reported a modified approach to resolve this issue of asymmetric reflections by using averaged value of reflection coefficients. The isotropic medium model cannot duplicate this property, as it is intrinsically symmetric, hence it is important to understand the EM dynamics of SR inspired NIM media, which inherently possess reflection asymmetric structures ($S_{11} \neq S_{22}$) [21].

II. EM DYNAMICS OF MEDIA

The fundamental equations describing characteristics of EM waves in a biaxial anisotropic medium (or simply called biaxial) are complex compared to isotropic equations. Isotropic materials have a single permittivity ϵ . In an isotropic

media, the constitutive relations that relate the electric flux density \vec{D} to the electric field intensity \vec{E} and the magnetic flux density \vec{B} to the magnetic field intensity \vec{H} are given by

$$\vec{D} = \epsilon \vec{E} = \epsilon_0 \epsilon_r \vec{E}; \vec{B} = \mu \vec{H} = \mu_0 \mu_r \vec{H} \quad (8)$$

From (8), the permittivity of the medium (ϵ) describes the medium's electrical properties and the permeability (μ) describes its magnetic properties. The time-harmonic forms of Maxwell's equations for isotropic media are given by

$$\nabla \times \vec{E} = -i\omega\mu\vec{H} \quad (9)$$

$$\nabla \times \vec{H} = i\omega\epsilon\vec{E} + \vec{J} \quad (10)$$

$$\nabla \cdot \vec{D} = \rho_v \quad (11)$$

$$\nabla \cdot \vec{B} = 0 \quad (12)$$

A medium is called electrically anisotropic if $\vec{D} = \bar{\epsilon} \cdot \vec{E}$, where $\bar{\epsilon}$ is the permittivity tensor. A medium is magnetically anisotropic if $\vec{B} = \bar{\mu} \cdot \vec{H}$, where $\bar{\mu}$ is the permeability tensor, note that \vec{B} and \vec{H} are no longer parallel. A medium can be both electrically and magnetically anisotropic.

In electrically anisotropic case \vec{D} and \vec{E} are no longer parallel, $\bar{\epsilon}$ is given by

$$\bar{\epsilon} = \begin{pmatrix} \epsilon_{xx} & \epsilon_{xy} & \epsilon_{xz} \\ \epsilon_{yx} & \epsilon_{yy} & \epsilon_{yz} \\ \epsilon_{zx} & \epsilon_{zy} & \epsilon_{zz} \end{pmatrix} \quad (13)$$

For example, crystals, in general, are described by a symmetric permittivity tensor; there always exist a coordinate transformation that transforms the symmetric matrix $\bar{\epsilon}$ to a diagonal matrix as given by

$$\bar{\epsilon} = \begin{pmatrix} \epsilon_{xx} & 0 & 0 \\ 0 & \epsilon_{yy} & 0 \\ 0 & 0 & \epsilon_{zz} \end{pmatrix} \quad (14)$$

From (14), new coordinate system is called the principal system, and the three coordinate axes are called the principal axes. For cubic crystal $\epsilon_{xx} = \epsilon_{yy} = \epsilon_{zz} = \epsilon = \epsilon_0 \epsilon_r$, the crystal is isotropic.

$$\bar{\epsilon} = \begin{pmatrix} \epsilon & 0 & 0 \\ 0 & \epsilon & 0 \\ 0 & 0 & \epsilon \end{pmatrix} = \epsilon_0 \begin{pmatrix} \epsilon_r & 0 & 0 \\ 0 & \epsilon_r & 0 \\ 0 & 0 & \epsilon_r \end{pmatrix} \quad (15)$$

For tetragonal, hexagonal, and rhombohedra crystals two of the three ϵ are equal, such crystal is called uniaxial.

Uniaxial anisotropic materials have two different permittivity values. Uniaxial materials have the same permittivity along two dimensions, and a different permittivity along the third dimension. The axis along the direction of the unique permittivity value is called the optic axis. An unrotated uniaxial permittivity tensor can be written as

$$\bar{\epsilon} = \begin{pmatrix} \epsilon & 0 & 0 \\ 0 & \epsilon & 0 \\ 0 & 0 & \epsilon_{zz} \end{pmatrix} \quad (16)$$

From (16), the principal axis that is different (exhibits anisotropy) is called the optical axis (z -axis is the optical axis), there exists a two dimensional degeneracy. If $\epsilon_{zz} > \epsilon$, the medium exhibits positive uniaxial behavior, and if $\epsilon_{zz} < \epsilon$, the medium shows negative uniaxial characteristics.

If $\epsilon_{xx} \neq \epsilon_{yy} \neq \epsilon_{zz}$, the crystal is biaxial, examples of biaxial crystals are orthorhombic, monoclinic, and triclinic. The defining property of electrically biaxial media is the permittivity tensor $\bar{\epsilon}$.

If the medium is biaxial anisotropic, the permittivity and permeability of medium acquire on a tensor form. From (8), the set of matrix equations can be described by

$$\bar{D} = \bar{\epsilon} \cdot \bar{E} = \epsilon_o \bar{\epsilon}_r \cdot \bar{E}; \bar{B} = \bar{\mu} \cdot \bar{H} = \mu_o \bar{\mu}_r \cdot \bar{H} \quad (17)$$

where $\bar{\epsilon}_r$ and $\bar{\mu}_r$ are relative permittivity and permeability tensors. From (17), the change in constitutive relations will also affect Maxwell's equations (9)-(12) in the medium, which can be described by

$$\nabla \times \bar{E} = -i\omega \bar{\mu} \bar{H} \quad (18)$$

$$\nabla \times \bar{H} = i\omega \bar{\epsilon} \bar{E} + \bar{J} \quad (19)$$

$$\nabla \cdot \bar{D} = \rho_V \quad (20)$$

$$\nabla \cdot \bar{B} = 0 \quad (21)$$

Since NIMs exhibit bianisotropic medium, provide coupling between electric and magnetic fields. The constitutive relations for a bianisotropic medium is given by

$$\bar{D} = \bar{\epsilon} \cdot \bar{E} + \bar{\xi} \cdot \bar{H} \quad (22)$$

$$\bar{B} = \bar{\mu} \cdot \bar{H} + \bar{\xi} \cdot \bar{E} \quad (23)$$

A bianisotropic medium placed in an electric or magnetic field becomes both polarized and magnetized. In general, any media in motion becomes bianisotropic. The simple example of bianisotropic materials are moving dielectrics and magnetic materials in the presence of electric or magnetic fields. The typical moving NIMs and their constitutive relations are the subject of the relativistic electromagnetic theory, can lead to repulsive Casimir effect (anti-gravity) [15]. The permittivity described in (16), represents an unrotated uniaxial medium with optic axis along the z-direction. Biaxially anisotropic materials have three unique values in the permittivity tensor and they have two optic axes. An unrotated biaxial permittivity tensor can be described by

$$\bar{\epsilon} = \begin{pmatrix} \epsilon_x & 0 & 0 \\ 0 & \epsilon_y & 0 \\ 0 & 0 & \epsilon_z \end{pmatrix} \quad (24)$$

where $\epsilon_x \neq \epsilon_y \neq \epsilon_z$. From (8), principal axes of a biaxial medium are aligned with the Cartesian coordinate system.

For clear understanding, Figure (5) shows the plots of the unrotated biaxial medium; the inner surface called as "a-wave vector surface" and the outer surface is the "b-wave vector surface" [10]. The intersecting line is one of the optic axes, it can be seen from Figure (5) that the optic axis intersects the wave vector surfaces at some point and the "b-wave wave vector surface" is at a local minimum at the point of intersection. If the biaxial medium is arbitrarily oriented with respect to the coordinate system, the permittivity tensor representation would be in complex form and not as a simple form described in (8).

The evaluation of the tensor for an arbitrarily oriented biaxial medium is given by applying rotations to the tensor in (8), the wave vector surfaces are shown in Figure (6).

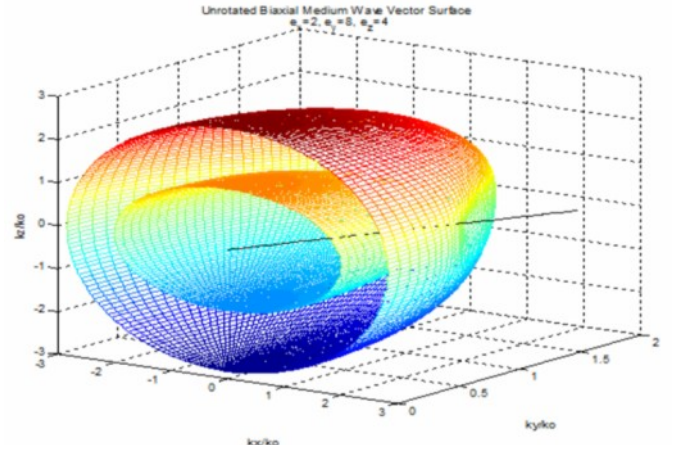


Fig. 5: Wave vector surface: unrotated biaxial medium $(\epsilon_x, \epsilon_y, \epsilon_z) = (2, 8, 4)$, plotted over: $0 \leq \theta \leq \pi, 0 \leq \phi \leq \pi$ [10]

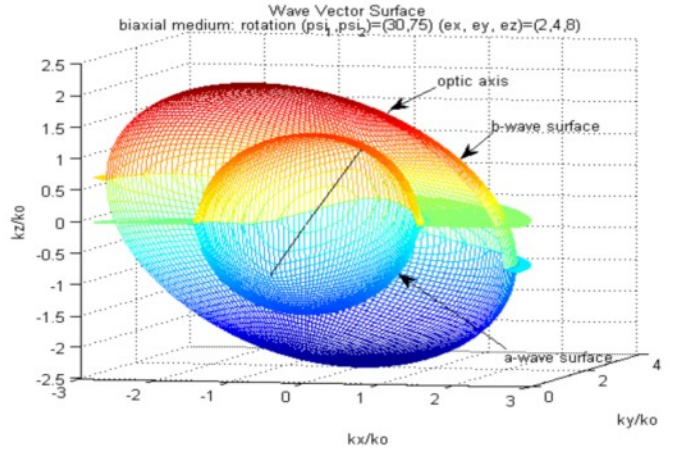


Fig.6: Wave vector surface: rotated biaxial medium $(\epsilon_x, \epsilon_y, \epsilon_z) = (2, 8, 4)$, rotated by $(\psi_1, \psi_2) = (30^\circ, 75^\circ)$ [10]

Studying the wave vector surfaces of the unbounded region as shown in Figures (5) and (6) give insight into how the wave influences the important medium parameters (ϵ, μ, n, z) in NIMS (negative index Möbius strips) structures, which fall into the category of anisotropic/bianisotropic because of geometry, topology, and orientations of their structure.

III. DETERMINATION OF CONSTITUTIVE PARAMETERS

Most of the NIMs presented over the past several years are artificially engineered Split Rings-inspired periodic structures [1]-[25]. It is convenient to extract the parameters from a unit cell of periodic SR (Split Ring) structures using numerical techniques. It has been demonstrated that under the condition of long wavelength the materials with periodic structures can be viewed as a homogeneous medium and their properties can be described by the effective medium parameters [1]-[5]. The properties of a periodic structure can be determined from the transfer-matrix (T) associated with the fields of a unit SR-cell.

NIMS (negative index Möbius Strips) structures are typically bianisotropic, hence cross-coupling exists between electric (E) and magnetic (H) fields because of their orientation, topology, and special geometry. When computing the effective parameters of NIMS structures, magneto-electric coupling dynamics cannot be disregarded. The simplified

approach to retrieve the coupling parameter of a bianisotropic material from S -parameters is based on transfer-matrix method. The transfer-matrix method has been used to retrieve the effective EM (electromagnetic) parameters of a homogeneous and non-homogeneous material [1]-[2].

Figure (7) shows a typical of bianisotropic slab of thickness “ d ”, placed in air, illustrates the direction of S (Scattering) parameters. For a material consisting of periodic structures, there exists a phase advance per unit cell, which can be defined by the periodicity [13]. Chen et al. [16] extracted effective constitutive parameters of bianisotropic negative index material from S -parameters for various wave polarizations using numerical approach for a plane wave polarized in the z direction and incident in the x direction.

Figure (8) shows the triplet $[\overline{k}_x, -\overline{H}_y, \overline{E}_z]$ based on RHS (right-handed coordinate system), containing electric (E) and magnetic (H) field. As shown in Figure (8), the plane wave polarized in z - axis propagates along the x -direction, the electric fields in the z -direction will induce magnetic dipoles and the magnetic fields in the y - direction will induce electric dipoles due to the asymmetry of the inner and outer rings. This implies that electric dipoles cannot only be excited by the E -fields but also by the H -fields. Similarly, magnetic dipoles cannot only be excited by the magnetic (H) fields but also by the electric fields (E) and vice-versa. Assuming that medium is reciprocal and that the harmonic time dependence is $e^{-i\omega t}$, constitutive relationship is given 19]

$$\overline{D} = \overline{\epsilon} \cdot \overline{E} + \overline{\xi} \cdot \overline{H} \quad (25)$$

$$\overline{B} = \overline{\mu} \cdot \overline{H} + \overline{\zeta} \cdot \overline{E} \quad (26)$$

$$\overline{\epsilon} = \epsilon_0 \begin{pmatrix} \epsilon_{xx} & 0 & 0 \\ 0 & \epsilon_{yy} & 0 \\ 0 & 0 & \epsilon_{zz} \end{pmatrix}, \quad \overline{\mu} = \mu_0 \begin{pmatrix} \mu_{xx} & 0 & 0 \\ 0 & \mu_{yy} & 0 \\ 0 & 0 & \mu_{zz} \end{pmatrix} \quad (27)$$

$$\overline{\xi} = \frac{1}{c} \begin{pmatrix} 0 & 0 & 0 \\ 0 & 0 & 0 \\ 0 & -i\xi_0 & 0 \end{pmatrix}, \quad \overline{\zeta} = \frac{1}{c} \begin{pmatrix} 0 & 0 & 0 \\ 0 & 0 & i\xi_0 \\ 0 & 0 & 0 \end{pmatrix} \quad (28)$$

where \overline{E} , \overline{H} , and \overline{D} , are electric field, magnetic field intensities, and flux densities; ϵ_0 and μ_0 are the permittivity and permeability of the vacuum; c is the speed of light in vacuum; and other four quantities are dimensionless and are unknowns. When a plane wave polarized in the z -direction incident in the x -direction, only 2-components of EM-fields (E_z and H_y) and 3-EM parameters (ϵ_{zz} , μ_{yy} , ξ_0) are included.

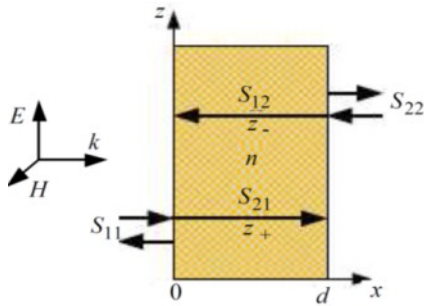


Fig.7. Plane wave incident in the x direction into a bianisotropic [13]

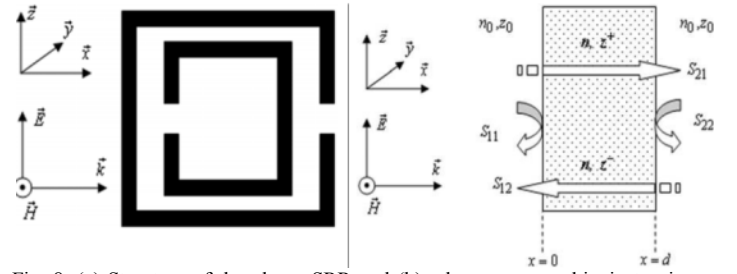


Fig. 8. (a) Structure of the planar SRR and (b) a homogeneous bianisotropic material slab with thickness d suspended in air and S -parameters used in the determination of the forward and backward wave impedances [3].

The numerical formulation is done for the determination of the forward and backward wave impedances entailed by parameters ϵ_{zz} , μ_{yy} and ξ_0 , since other unknown four quantities ϵ_{xx} , ϵ_{yy} , μ_{xx} , and μ_{zz} are not related to the bianisotropic structure in Figure 8(b).

From (18)-(19):

$$\frac{\partial^2 E_z}{\partial x^2} + k_x^2 E_z = 0, \quad \frac{\partial^2 H_y}{\partial x^2} + k_x^2 H_y = 0 \quad (29)$$

$$Z^+ = \frac{E^+}{H^+} = Z_0 \frac{\mu_{yy}}{(n+i\xi_0)} \quad (30)$$

$$Z^- = \frac{E^-}{H^-} = Z_0 \frac{\mu_{yy}}{(n-i\xi_0)}, \quad Z_0 = \sqrt{\frac{\mu_0}{\epsilon_0}} \quad (31)$$

$$z^\pm = Z^\pm / Z_0; \quad z^+ = Z^+ / Z_0; \quad z^- = Z^- / Z_0 \quad (32)$$

$$k_x^2 = k_0^2 (\epsilon_{zz} \mu_{yy} - \xi_0^2), \quad k_x = n k_0 \quad (33)$$

$$n^2 = \epsilon_{zz} \mu_{yy} - \xi_0^2, \quad n = \pm \sqrt{\epsilon_{zz} \mu_{yy} - \xi_0^2} \quad (34)$$

where E_z and H_y are the z and y components of \overline{E} and \overline{H} ; k_x and k_0 are the wave number of the wave propagating in the x direction and in free-space, Z^+ and Z^- are wave impedances inside the medium for forward ($+\hat{x}$) and backward ($-\hat{x}$) propagations; z^+ and z^- are normalized wave impedances in respective directions; Z_0 is the wave impedance (or intrinsic impedance) in air; and n is the refractive index of the negative index structure.

From (30)-(31), bianisotropic NIM (negative index material) structure samples exhibit different values of wave-impedances for forward and backward wave propagating direction [2, 20]. It is to note that non-homogeneous periodic NIM structure does not exhibit distinct impedance values because ratio of E/\overline{H} will vary periodically throughout the structure. This variation is negligible if the NIM structure unit cell sizes are small relative to the wavelength. The real challenge is the lack of a unique definition for z^\pm indicates that the values of ϵ and μ retrieved are not assignable. Within acceptable error limit, they can be applied if the NIM formed by periodic structure terminated always in the same location of the unit cell. However, the surface termination has an increasing influence on the scattering properties of the structure as the scale of inhomogeneity increases relative to the wavelength. It has been demonstrated that under the condition of long wavelength the materials with periodic structures can be viewed as a homogeneous medium and their

properties can be described by the effective medium parameters. The properties of a periodic structure can be determined from the transfer-matrix (T) which associated with the fields of a unit cell. We express the fields in the form of a vector $F = \bar{F} = (\bar{E}, \bar{H})^T$, where \bar{E} and \bar{H} are the complex amplitudes of the electric and magnetic fields located on the LH (left-hand) and RH (right-hand) faces of a slab. The magnetic field is a reduced field with the normalization form $\bar{H}' = i\omega\mu\bar{H}$. The relations of fields on two sides of a slab can be expressed as

$$\bar{F}(x+d) = e^{i\alpha d}\bar{F}(x) = T\bar{F}(x) \quad (35)$$

where α is the phase advance per unit cell which relates the fields on the two sides of a unit cell. T is the one dimensional transfer matrix of a NIM slab

$$T = \begin{pmatrix} T_{11} & T_{12} \\ T_{21} & T_{22} \end{pmatrix} = \begin{pmatrix} \cos(nk_0d) & -\frac{z}{k_0}\sin(nk_0d) \\ \frac{z}{k_0}\sin(nk_0d) & \cos(nk_0d) \end{pmatrix} \quad (36)$$

with k_0 being the wave number of light in free space, z being the wave impedance of a slab and n being the refractive index. From (35) and (36), dispersion relation is given by solving

$$T_{11}T_{22} - e^{i\alpha d}(T_{11} + T_{22}) + e^{i2\alpha d} - T_{12}T_{21} = 0 \quad (37)$$

The elements of the transfer matrix can be expressed in terms of S parameters

$$T_{11} = \frac{(1+S_{11})(1-S_{22})+S_{21}S_{12}}{2S_{21}} \quad (38)$$

$$T_{12} = \frac{(1+S_{11})(1+S_{22})-S_{21}S_{12}}{2S_{21}} \quad (39)$$

$$T_{21} = \frac{(1-S_{11})(1-S_{22})-S_{21}S_{12}}{2S_{21}} \quad (40)$$

$$T_{22} = \frac{(1-S_{11})(1+S_{22})+S_{21}S_{12}}{2S_{21}} \quad (41)$$

Figure (9) shows the schematic of a typical homogeneous bianisotropic material slab that is placed in an open space. There are two different situations to be considered, i.e., wave incidence in the $+x$ and $-x$ directions. After applying the boundary continuous conditions, it is straightforward to obtain the expressions for the S parameters by using the transfer matrix method [20]. When the incidence is in the $+x$ direction as shown in Figures (7) and (9a), the corresponding reflection (S_{11}) and transmission (S_{21}) coefficients are as

$$S_{11} = \frac{2i \sin(nk_0l)[n^2 + (\xi_0 + i\mu_y)^2]}{[(\mu_y + n)^2 + \xi_0^2]e^{-ink_0l} - [(\mu_y - n)^2 + \xi_0^2]e^{ink_0l}} \quad (42)$$

$$S_{21} = \frac{4\mu_y n}{[(\mu_y + n)^2 + \xi_0^2]e^{-ink_0l} - [(\mu_y - n)^2 + \xi_0^2]e^{ink_0l}} \quad (43)$$

where l is the thickness of the homogeneous bianisotropic material slab and k_0 is the wave number of light in free space. For the case, when the incidence is in the $-x$ direction, as shown in Figure (9b), we obtain the corresponding reflection (S_{22}) and transmission (S_{12}) coefficients as

$$S_{12} = \frac{4\mu_y n}{[(\mu_y + n)^2 + \xi_0^2]e^{-ink_0l} - [(\mu_y - n)^2 + \xi_0^2]e^{ink_0l}} \quad (44)$$

$$S_{22} = \frac{2i \sin(nk_0l)[n^2 + (\xi_0 - i\mu_y)^2]}{[(\mu_y + n)^2 + \xi_0^2]e^{-ink_0l} - [(\mu_y - n)^2 + \xi_0^2]e^{ink_0l}} \quad (45)$$

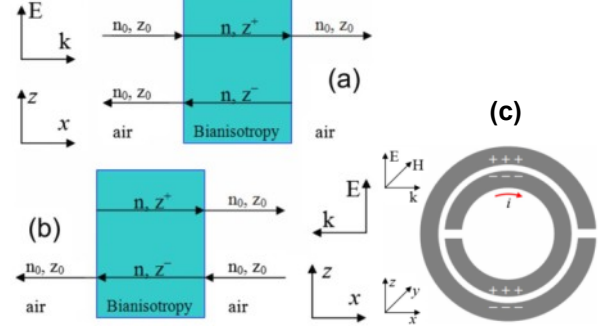


Fig.9. Schematics of a homogeneous bianisotropic slab placed in open space for the calculation of S parameters: (a) and (b) are for plane wave's incident in the $+x$ and $-x$ directions, respectively, (c) NMIS unit cell.

From (43)-(45), S_{21} is equal to S_{12} , but S_{11} is not equal to S_{22} . There are 3-independent equations to for the 3-unknowns (n , μ_{yy} and ξ_0). By solving analytically (43)-(45), the expression for refractive index n is given by

$$\cos(nk_0d) = \cos(\alpha d) = \frac{1-(S_{11}S_{22})+S_{21}^2}{2S_{21}} \quad (46a)$$

From (36), using the condition of determinant (T) = 1, and substituting (38)-(41):

$$\cos(nk_0d) = \cos(\alpha d) = \frac{1-(S_{11}S_{22})+S_{21}^2}{2S_{21}} \quad (46b)$$

It is implicit that when S_{11} is equal to S_{22} , (46) will degenerate into a standard retrieval form [2]. The refractive index n can be obtained from the implicit expression (46), which has many solutions for n to the different branches of the inverse cosine. When solving for n from (46), one must determine one branch from many branches of solutions. For a passive medium, solution of n must obey the condition $n'' = \text{Im}(n) \geq 0$, after computing n , other constitutive parameters is given as

$$\xi_0 = \left(\frac{n}{-2 \sin(nk_0l)} \right) \left(\frac{S_{11}-S_{22}}{S_{21}} \right) \quad (47)$$

$$\mu_y = \left(\frac{in}{\sin(nk_0l)} \right) \left(\frac{2+S_{11}+S_{22}}{2S_{21}} - \cos(nk_0l) \right) \quad (48)$$

$$\epsilon_z = \left(\frac{n^2 + \xi_0^2}{\mu_y} \right) \quad (49)$$

Consequently, impedances z_+ and z_- can be obtained from (29)-(30). For a passive medium, following conditions should be satisfied $z_+ = \text{Re}(z_+) \geq 0$, $z_- = \text{Re}(z_-) \geq 0$.

From (47)-(49), retrieved effective constitutive parameters can be assigned to NIM structure with a minimum errors. However, variety of artifacts exists in the retrieved material parameters that are related to the inherent inhomogeneity of the NIM structure. The artifacts in the retrieved material parameters are particularly severe for NIM structure that make use of resonant elements, as large fluctuations in the index and impedance can occur, such that the wavelength within the material can be on the order of or smaller than the unit cell dimension. The retrieval technique based on analyzing the S-parameter of a finite slab can suffer from unphysical anti-resonances with a negative imaginary part for some of the parameters; these anomalies could be due to periodicity of the structure and spatial dispersion [11]-[12].

An example of this behavior can be seen in the retrieved imaginary parts of ϵ and μ , which typically differ in sign for a unit cell that has a magnetic or an electric resonance. In homogeneous passive media, the imaginary components of the material parameters are restricted to positive values. This anomalous behavior vanishes as the unit cell size approaches zero [2]. For a homogeneous or symmetric material, the value of z will be unique, while it will result in two different values for an inhomogeneous or asymmetric material. The impedance z is an intrinsic parameter which relates the electric field to the magnetic field as $= \frac{\vec{E}}{\vec{H}'}$. From (35), two equivalent expressions for the impedance of a slab can be obtained by

$$z = \frac{T_{12}}{e^{i\alpha d} - T_{11}} = \frac{e^{i\alpha d} - T_{22}}{T_{21}} \quad (50)$$

From (37) and (50)

$$Z^\pm = \pm \frac{(T_{11} - T_{22}) \pm \sqrt{(T_{22} - T_{11})^2 + 4T_{12}T_{21}}}{2T_{21}} \quad (51)$$

From two roots of (51) correspond to the two propagation directions of a plane wave. Substitution of (38)-(41) into (50) leads to

$$Z^\pm = \pm \frac{(S_{11} - S_{22}) \pm \sqrt{(1 - S_{11}S_{22} + S_{12}S_{21})^2 - 4S_{12}S_{21}}}{(1 - S_{11})(1 - S_{22}) - S_{12}S_{21}} \quad (52)$$

From (51) and (52), characteristic impedance which associates with a metamaterial with bianisotropic structures in terms of S parameters. For a passive medium the impedance needs to satisfy the conditions $(z^+)' \geq 0$ and $(-z^-)' \geq 0$, where $(\cdot)'$ denotes the real part operator.

For an example, a typical array of SRRs (split ring resonators) printed on substrate, and unit cell is shown in Figure (10). As illustrated in Figure (10a), a plane wave is incident in the x direction and polarized in the z direction. For numerical example, the dimensions as $a = 3$ mm, $r = 0.74$ mm, $c = 0.2$ mm, $s = 0.1$ mm, $g = 0.2$ mm, $t = 0.3$ mm, $h = 35$ mm; and permittivity of the substrate is ϵ_0 for simplification [13]. It can be seen from Figures (10b) and (10c) that S_{12} is equal to S_{21} and the magnitudes of S_{11} and S_{22} are almost the same, while the phase of S_{11} is different with that of S_{22} . In this case, the application of the standard retrieval method [1] will lead to an inaccurate result.

The discrepancy in phase of S parameter measurement is because of the fact that the NIM's cells are not infinitely small compared to the incoming wavelength, causing space dispersion. Assuming that there is a plane wave propagating in the direction of $+x$, polarized in the $+z$ direction. The constitutive relationship between electric field and magnetic field can be described as

$$\vec{D}_z = \epsilon_0 \epsilon_z \vec{E}_z - ic^{-1} \xi_0 \vec{H}_y \quad (53)$$

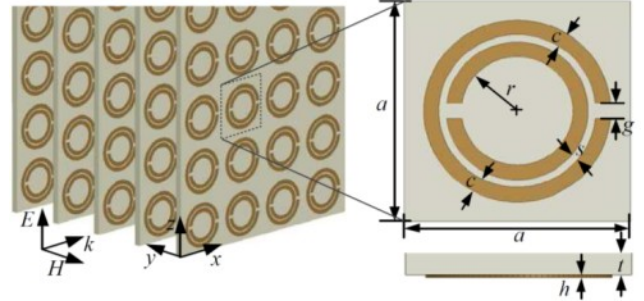
$$\vec{B}_y = \mu_0 \mu_y \vec{H}_y + ic^{-1} \xi_0 \vec{E}_z \quad (54)$$

With the substitution of (53)-(54) into Maxwell's equations (18)-(19):

$$\nabla^2 \vec{E}_z + \omega^2 \epsilon_0 \mu_0 (\epsilon_z \mu_y - \xi_0^2) \vec{E}_z = 0 \quad (55)$$

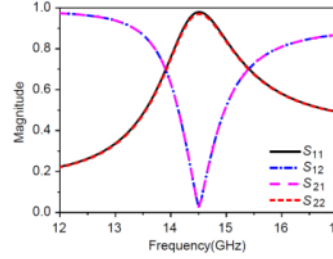
From (13), the index (n) can be given by

$$n^2 = \epsilon_z \mu_y - \xi_0^2 \quad (56)$$

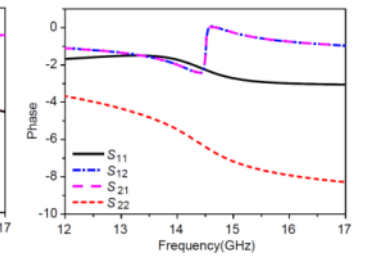


(a) Array of SRRs printed on substrate

(b) SRR unit cell



(c) Magnitude: S-parameters



(d) Phase: S-parameters

Fig.10: A typical bianisotropic structure: (a) array of SRRs printed on substrate with the metallization in yellow, (b) SRR unit cell, (c) magnitude of S-parameters, and (d) phase of S-parameters [13]

For a passive material, the roots have to be chosen properly to guarantee the condition $Im(n) \geq 0$. Otherwise, the exponentially growing solutions will occur, which violates the energy conservation. The impedances of a bianisotropic material for the wave propagation in the right-hand or left-hand directions are Z^\pm , the values of which are given by the equations $Z^+ = \frac{E^+}{H^+}$ and $Z^- = \frac{E^-}{H^-}$. From Maxwell's equations (18)-(21), the formulas of the impedance and effective parameters s can be obtained,

$$Z^\pm = \frac{Z^\pm}{Z_0} = \frac{\mu_y}{\pm n - i\xi_0}, Z_0 = \sqrt{\frac{\mu_0}{\epsilon_0}} \quad (57)$$

$$\epsilon_z = \frac{n + i\xi_0}{Z^+} \quad (58)$$

$$\mu_y = (n - i\xi_0)Z^+ \quad (59)$$

$$\xi_0 = in \frac{Z^- + Z^+}{Z^- - Z^+} \quad (60)$$

The refractive index of and impedances for a bianisotropic medium can be obtained from (46) and (52). The expressions for the effective electromagnetic parameters (ϵ_z , μ_y and ξ_0) and impedance associate with the bianisotropic structure such as are given from (58)-(60), can be used for designing NIMS resonator for next generation energy efficient signal sources.

IV. NIMS INSPIRED RESONATOR FOR OSCILLATOR CIRCUIT

NIMs resonator can be classified into two types: resonant type and non-resonant type: examples are Split Ring Resonator (SRR), and Left Handed (LH) Transmission Line (T-line). Resonant type metamaterial exhibit larger dynamic range for material parameter ($\epsilon_r < 0$, $\mu_r < 0$), while non-resonant type offers wide bandwidth and lower loss. Traditional metamaterial transmission lines (T-lines) can also be categorized into

resonant type and non-resonant type, represented by (split-ring-resonator) SRR/(complementary split-ring-resonator) CSRR loaded T-line, and Composite Right/Left Handed (CRLH) T-line, with the corresponding layout shown in Figures (11) and (12), where C and L are per-unit length capacitance and inductance that determine the metamaterial properties of T-lines. For T-line loaded with SRR (Fig. 1), L_1 and C_2 linked with T-line, whereas C_1 and L_2 are linked to magnetic coupling.

Figure (11) shows the typical split ring resonator and the construction of NIM. The physical properties of Figure (11) are given by:

$$\varepsilon = \frac{Y}{j\omega} = C_2 \text{ is } +ve \rightarrow \varepsilon > 0 (+ve) \quad (61)$$

$$\mu = \frac{Z}{j\omega} = \frac{L_1+L_2-\omega^2 L_1 L_2 C_1}{1-\omega^2 L_2 C_1} \quad (62)$$

$$\mu < 0 (-ve) \text{ for } \left(\frac{1}{L_2 C_1}\right)^{1/2} < \omega < \left(\frac{L_1+L_2}{L_1 L_2 C_1}\right)^{1/2} \quad (63)$$

From (61) and (63), $\text{Re}(\mu)$ is negative and $\text{Re}(\varepsilon)$ is positive. For ($\varepsilon > 0$, $\mu < 0$), propagating waves become evanescent waves, therefore energy cannot propagate through the resonator, reflected back to establish a standing-wave.

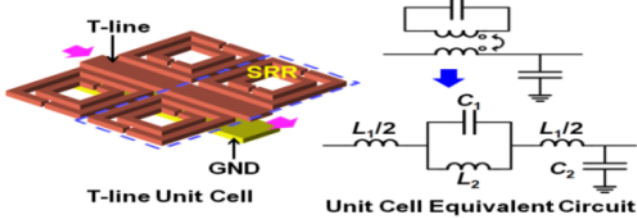


Fig.11: SRR loaded T-line unit cell and equivalent lumped LC model

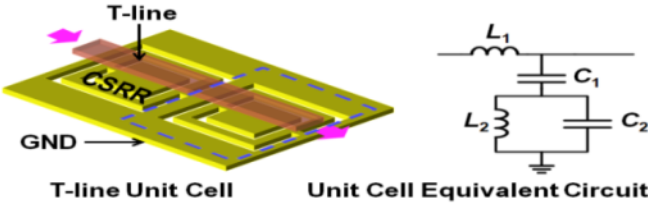


Fig.12: CSRR loaded T-line unit cell and equivalent lumped LC model

As a result, SRR loaded T-line structure stores the energy and forms a high-Q resonator tank circuit for low phase noise oscillator application. Similarly, for T-line loaded with CSRR (Fig. 12), L_1 associated with T-line, C_1 , C_2 , and L_2 account from electric coupling of CSRR on the ground. The physical properties of Figure (12) are given by

$$\mu = \frac{Y}{j\omega} = L_1 \text{ is } +ve \rightarrow \mu > 0 (+ve) \quad (64)$$

$$\varepsilon = \frac{Y}{j\omega} = \frac{C_1(1-\omega^2 L_2 C_2)}{1-\omega^2(C_1+C_2)L_2} \quad (65)$$

$$\varepsilon < 0 (-ve) \text{ for } \left(\frac{1}{(C_1+C_2)L_2}\right)^{1/2} < \omega < \left(\frac{1}{L_2 C_2}\right)^{1/2} \quad (66)$$

From (64) and (66), $\text{Re}(\mu)$ is positive and $\text{Re}(\varepsilon)$ is negative, In this case ($\varepsilon < 0$, $\mu > 0$), electric plasma is formed, where propagating waves become evanescent waves, hence, energy cannot propagate through the resonator either and is reflected back to establish a standing-wave. As a result, CSRR loaded T-line can also be used to form a high-Q resonator.

Figure 13(a) shows the structure of the broadside-coupled split-ring resonator, there are two relative slips S_x and S_y between the two broadsides coupled rings. Figure 13(b) shows the corresponding equivalent circuit, where L, R are the equivalent inductance and resistance, respectively; C_0 is mutual capacitances between the two rings; C_s is the capacitance of the split. As shown in Figure (13a), the tuning can realize by minor slips along and perpendicular to the gap direction of two broadsides coupled rings [22].

Figure (14) shows the (a) layout of the broad coupled split ring (dark region denotes etched on signal plane, and light region denotes broadsides coupled triangular SR etched on ground plane), and (b) equivalent lumped circuit.

For the validation of reported research work, resonators were fabricated on low loss Quartz and Borosilicate material. As shown in Fig. (3), the metal structures are processed on top of quartz wafers (diameter $D=150$ mm). The fabrication process uses a double-side coating of the substrates using a metallization, sputtered metal gold (Au) is used.

Unlike SRR/CSRR as depicted in Figure (15), the geometry of Negative Index Möbius-Strips (NIMS) is conformal, continuous, and maps one-to-one onto itself. These unique properties of NIMS permit EM coupling in such a way that signal coupled to loop does not encounter any obstructions when travelling around the loop, emulate like an infinite transmission line, hence large group delay and high Q-factor. In this paper, oscillator circuit uses negative index ($\varepsilon_r < 0$, $\mu_r < 0$) NIMO (Negative Index Möbius Oscillator) circuit for low cost high performance solution.

V. EXAMPLES & VALIDATION

The novel NIMO (Negative Index Möbius Oscillator) circuit shown in Figures (16) is built on substrate (8-mill thick), uses BFP740 SiGeHBT transistor for providing negative resistance to compensate the losses of the resonator tank. The total DC power consumption is 680 mW that includes the buffer amplifier; operates at 8Volt and 85mA.

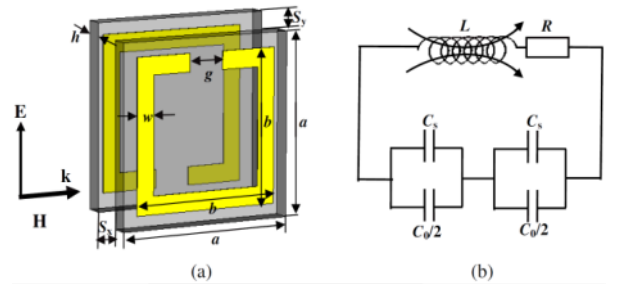


Fig.13: (a) A broadside-coupled split-ring resonator (b) equivalent circuit [22]



Fig.14: (a) Layout of the BCTSR (dark region denotes BCTSR etched on signal plane, and light region denotes broadsides coupled triangular SR etched on ground plane) (b) equivalent lumped circuit

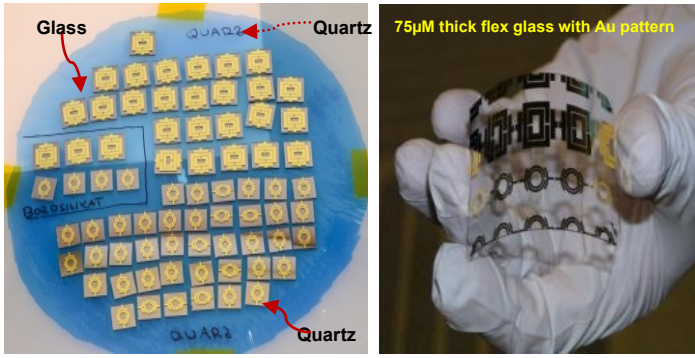


Fig.15: Photos of metamaterial resonator fabricated on glass/quartz

Figure (16) shows the typical circuit schematic of 28.5 GHz tunable NIMO circuit that uses NIMS resonator as a tank network for improving evanescent mode coupled energy of the resonator tank module and coupled SRR for mode-locking and unwanted mode suppression. Figure (17) shows the measured phase noise plot is -144 dBc/Hz @ 100 kHz offset with 10.56 dBm output power. The measured FOM (figure of merit) @ 1MHz is -226 dBc/Hz for a given 680 mW DC power consumption. The main drawback of this configuration is limited tuning (< 5%) to compensates the frequency drift due to change in temperature.

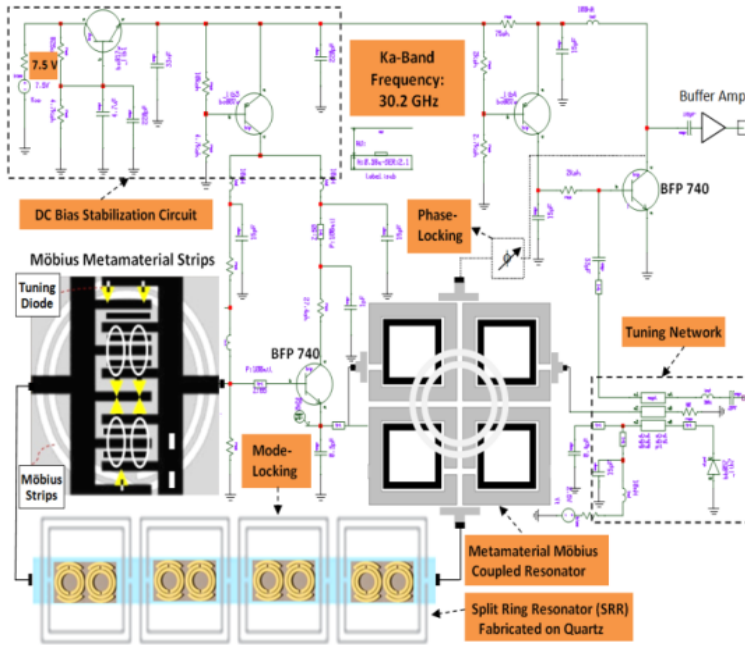


Fig.16: 28.5 GHz NIMO circuit ($\epsilon_r = 2.2$, thick, 8-mil)

Table 1: Recent published oscillator's performance and this work

References	f_o GHz	P_{DC} mW	P_o dBm	Tuning GHz	$L(f)$ dBc/Hz	FOM dBc/Hz
[23]	22.1	11.1	-11	20.6%	-109	-181
[24]	11.16	20	2.9	4.1%	-125.1	-193
[25]	12.4	30	7	2.5%	-122	-189.1
[26]	38.06	129.9	10.46	2.6%	-112.3	-182.7
[27]	28.33	15	0.3	-	-98.5	-176.4
This work Fig.16	28.5	680	10.56	1.8%	-166.9	-226.7

For practical applications, tuning range need to be improved. The tuning capability of NIMO circuit shown in Figure (16) is enhanced by incorporating phase-stabilization (manipulating the phase velocity by introducing Mode-Suppression Ring that allows multi-mode-phase-injection into the Möbius-Strips cavity), enabling Q-multiplier effect and exponential rise in Q-factor over the desired tuning range.

Table 1 shows the recent published papers and compares this work based on FOM.

VI. CONCLUSION

The reported NIMO topology enables next generation energy efficient signal source solutions in integrated circuit and surface mounted planar technology.

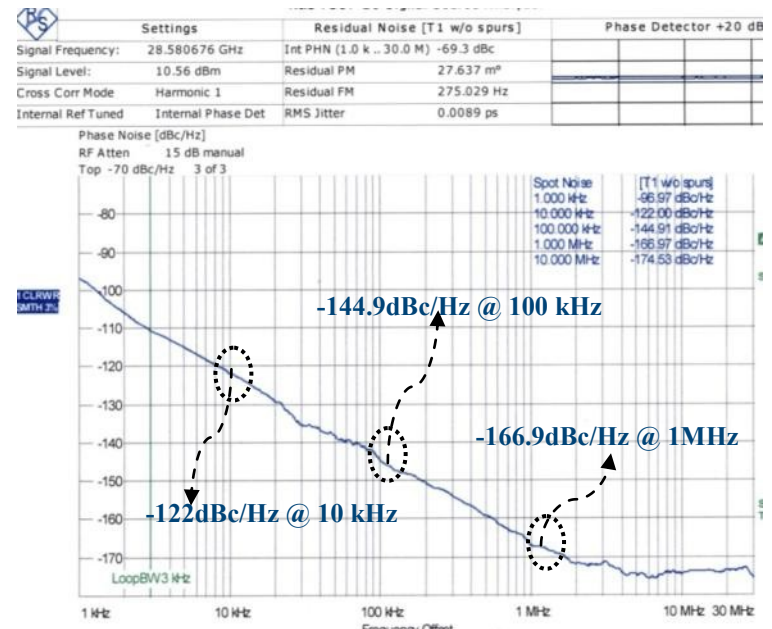


Fig. 17: Measured Phase Noise plot of 28.5 GHz NIMO (Fig. 16)

REFERENCES

- [1] Smith et al, "Determination of effective permittivity and permeability of Metamaterials from reflection and transmission coefficients," *Phys.Rev. B*, Vol. 65, No. 19, 195104, 2002
- [2] Smith et al, "Electromagnetic parameter retrieval from inhomogeneous Metamaterials," *Phys. Rev. E*, Vol. 71, No. 3, 36617, 2005.
- [3] U. C. Hasar and J. J. Barroso, "Retrieval approach for determination of forward and backward wave impedances of bianisotropic Metamaterials", *PIER*, Vol. 112, pp. 109-124, 2011
- [4] Pendry et al, "Low frequency plasmons in thin-wire structures", *J. Phys.:Condens. Matter*, Vol. 10, No. 22, pp. 4785-4809, Jun. 1998.
- [5] Marques et al, "Role of bianisotropic in negative permeability and left-handed metamaterials", *Phys. Rev. B*, Vol. 65, pp. 144440-1-6, 2002.
- [6] Nicolson, A. M. and G. Ross, "Measurement of the intrinsic properties of materials by time-domain techniques", *IEEE Trans. Instrum. Meas.* Vol. 19, No. 4, 377-382, 1970.
- [7] Weir, W. B., "Automatic measurement of complex dielectric constant and permeability at microwave frequencies," *Proc. IEEE*, Vol. 62, No. 1, 33-36, 1974.
- [8] Milosevic et al, "Effective Electromagnetic Parameters of Metamaterial Transmission Line Loaded With Asymmetric Unit Cells", *IEEE Trans. on MTT*, Vol. 61, No. 8, pp. 2761-2772, Au. 2013

- [9] Landau et al “Electrodynamics of Continuous Media”, 2nd ed. Oxford, U.K.: Pergamon, 1984.
- [10] J. W. Graham, “Arbitrary oriented biaxial anisotropic media: wave behaviors and microstrip antennas”, PhD Dissertation, Syracuse University, May 2012
- [11] Koschny et al, “Impact of inherent periodic structure on effective medium description of left-handed and related Metamaterials,” *Phys. Rev. B, Condens. Matter* vol. 71, Jun. 2005.
- [12] A. Alù, “Restoring the physical meaning of metamaterial constitutive Parameters,” *Phys. Rev. B, Condens. Matter* vol. 83, Feb. 2011
- [13] Chen et al, “Determining the effective electromagnetic parameters of bianisotropic Metamaterials with periodic structures”, *PIERM*, Vol. 29, pp. 79-93, 2013
- [14] Chen et al, “Robust method to retrieve the constitutive effective parameters of Metamaterial”, *Phys. Rev. E*, Vol. 70, No. 1, 16608, 2004.
- [15] Ulrich L. Rode, Ajay K. Poddar, “Möbius Metamaterial inspired next generation circuits and systems”, *Microwave Journal*, May 2016
- [16] Chen et al, “Retrieval of the effective constitutive parameters of bianisotropic Metamaterial”, *Phys. Rev. E*, Vol. 71, 046610–9, 2005.
- [17] Marques et al, “Metamaterial with Negative Parameters: Theory, Design and Microwave Applications, Wiley, 2008.
- [18] Sydoruk et al, “Analytical formulation for the resonant frequency of split rings”, *J. Appl. Phys.*, Vol. 105, No. 1, 14903, 2009.
- [19] Chen et al, “Optimization approach to the retrieval of the constitutive parameters of a slab of general bianisotropic medium”, *PIERS*, Vol. 60, 1-18, 2006.
- [20] Li ET AL, “Determination of the effective constitutive parameters of bianisotropic Metamaterials from reflection and transmission coefficients,” *Phys. Rev. E*, Vol. 79, 026610-1-7, 2009.
- [21] Hasar, U. C., “Procedure for accurate and stable constitutive parameters extraction of materials at microwave frequencies”, *PIERS*, Vol. 109, 107-121, 2010.
- [22] Wang ET AL, “A tunable left-handed metamaterial based on modified broadside-coupling split-ring resonators”, *PIERS Letters*, Vol. 6, pp. 35–45, 2009
- [23] Nakamura et al, “A 11.1-V Regulator-Stabilized 21.4-GHz VCO and a 11.5% Frequency-Range dynamic divider for K-Band wireless communication”, *MTT-Trans*, vol.60, No. 9, pp. 2823-2832, Sept. 2012.
- [24] Chen et al, “Design of high-Q tunable SIW resonator and its application to low phase noise VCO,” *IEEE Microw. Wireless Compon. Lett.*, vol. 23, no. 1, pp. 43–45, Jan. 2013.
- [25] Collado et al, “Mechanically Tunable Substrate Integrated Waveguide (SIW) Cavity Based Oscillator”, *IEEE MWCL*, vol. 23, no. 9, pp. 489–491, Sep. 2013.
- [26] Chang et. al., “A new monolithic Ka-Band Filter-based voltage controlled oscillator using 0.15 μ m GaAs PHEMT Technology”, *IEEE MWCL Letters*, pp. 111-113, Vol. 24, No. 2, Feb 2014.
- [27] Chen et.al., “Design of X-band and Ka-band Colpitts oscillators using a parasitic cancellation technique”, *IEEE Trans.Circuits System-I*, Vol. 57, pp. 1817-1828, Aug 2010